ELSEVIER

Journal of Nuclear Materials 264 (1999) 206–215

journal of nuclear materials

Corrosion behavior of Mo–Re based alloys in liquid Li

Jun-ichi Saito [a,*], Masahiko Morinaga [b], Shigeki Kano [a], Mitsuaki Furui [b], Kenji Noda [b]

[a] *Oarai Engineering Center, Power Reactor and Nuclear Fuel Development Corporation, 4002 Narita, Oarai-machi, Higashi-Ibaraki-gun, Ibaraki 311-1393, Japan*

[b] *Department of Materials Science and Engineering, School of Engineering, Nagoya University, Furo-cho, Chikusa-ku, Nagoya, Aichi 464-8063, Japan*

Received 19 January 1998; accepted 12 June 1998

Abstract

The corrosion behavior was investigated in liquid Li at 1473 K for 1.8 Ms using a capsule test for two Mo–Re based alloys, Mo–15mol%Re–0.1mol%Zr and Mo–15mol%Re–0.1mol%Zr–0.1mol%Ti. They showed mass gains due to the corrosion. The amount of mass gains increased with increasing corrosion time. Two types of corrosion products were formed on the surface of them. One was Re_2Zr and the other was ZrN according to the analyses using X-ray diffraction method and Auger electron spectroscopy. A deposition mechanism of these compounds was proposed on the basis of the experimental results. However, despite the appearance of these compounds, there were not any cracks on the surface even after the corrosion test for 1.8 Ms. From these results, these alloys were found to exhibit superior corrosion resistance against liquid Li.

PACS: 28.41.Qb; 81.65.Kn

1. Introduction

Molybdenum and Mo-based alloys possess excellent mechanical properties such as high tensile strength and very high creep strength at high temperatures [1–3], and hence they are suitable materials for high-temperature structural applications. For example, in advanced nuclear power plants, new structural materials which are superior in the mechanical and corrosion properties to the conventional materials, are desired strongly for raising thermal efficiency and also for securing the safety of the plant system during a long term service at high temperatures. For these materials which are serviced in the severe environment of alkali metal-cooled fast breeder reactor (FBR), good compatibility is first required with liquid alkali metal. Namely, corrosion resistance against alkali metal such as Li and Na is one of the most important properties for use of the material for such applications. Here, the liquid Li is more beneficial for the coolant than the liquid Na, because of its high boiling temperature and larger specific heat than Na.

There were a few investigations on the corrosion property of pure Mo and Mo-based alloys in liquid Li. Katsuta et al. [4] carried out the corrosion tests of pure Mo and TZM (Mo–0.5wt%Ti–0.1wt%Zr–0.01wt%C) in liquid Li at 873 K for 1018 h (3.66 Ms), and showed that the corrosion rates of Mo and TZM were 2 and 5 mm/yr, respectively. Also, DiStefano [5] reported that the mass change was $-0.011 g/cm^2$ for pure Mo tested in liquid Li at 1270 K for 400 h (1.44 Ms). Thus, Mo and Mo-based alloys have excellent corrosion resistance in liquid Li. Recently, Inoue et al. [6] have investigated the corrosion behavior of Nb-based and Mo-based alloys in liquid Li, and shown that Mo-based alloys have more excellent corrosion resistance than Nb-based alloys. It is also known that the corrosion rate of refractory metals and their alloys in liquid Li is affected by the existence of nonmetallic impurities in both liquid Li and metals and alloys [7–9]. However, such an impurity effect on the

* Corresponding author. E-mail: saito@oec.pnc.go.jp.

0022-3115/99/$ – see front matter
PII: S0022-3115(98)00459-0

corrosion is less dominant in Mo-based alloys than in Nb-based alloys.

In this study, corrosion tests were carried out with two Mo–Re based alloys in liquid Li at 1473 K for 1.8 Ms. These two alloys were designed in view of cold-workability, weldability and corrosion resistance in liquid Li [10,11], as explained later. The corrosive surface of them was observed using optical microscopy. The corrosion products on the surface were also analyzed with the X-ray diffraction method and the Auger electron spectroscopy (AES). Furthermore, a deposition mechanism of corrosion products on the surface was discussed on the basis of the present experimental results.

2. Experimental procedure

2.1. Specimen preparation

The nominal compositions are shown in Table 1 for two Mo–Re based alloys used in the present experiment. Both the mechanical property at room temperature and the weldability are improved by the Re addition into Mo [12,13]. The ductility at room temperature and corrosion resistance in liquid Li are probably improved by the addition of small amounts of Zr and Ti into Mo [14]. The amounts of the respective alloying elements in the alloys were chosen so as to optimize their mechanical properties.

These alloys were produced using the powder-metallurgy technique. The production process is shown in Fig. 1. Subsequent to sintering and forging, hot-rolling was performed at 1473 K so that the thickness reduction was over 95%, and then followed by cutting. Final heat treatment was carried out at 1773 K for 3.6 ks in vacuum. The specimens for corrosion test were then cut into the size of 10 mm square and 2 mm thick. The specimen surface was polished mechanically with a #1200 emery paper. Four test pieces were prepared for each alloy in order to check the reproducibility of experimental data.

2.2. Corrosion test

A series of corrosion tests was performed by setting the specimens in a capsule which was filled with liquid Li and subsequently by heating it at 1473 K for 1.8 Ms. The test apparatus used in the present experiment was the same as that used previously [15]. Twelve specimens were able to be tested at the same time in this equipment. The inner capsule was set inside the outer capsule. This system of double capsules, which are made of Nb–1wt%Zr, guarantees against the leakage of liquid Li to the outside of the system. The chemical composition of Nb–1wt%Zr which was used for both capsule and holder was shown in Table 2. Every operation for setting-up and taking-out of specimens was performed in the high purity Ar gas atmosphere in a glove-box. The gas concentrations of O_2, N_2 and H_2O in the glove-box were controlled so that the oxygen concentration <1 ppm, the nitrogen concentration <29 ppm and the moisture concentration <3 ppm. During the corrosion test at 1473 K, the capsule system was held in a high purity Ar gas atmosphere. The chemical composition of liquid Li analyzed prior to the corrosion test is shown in Table 3.

Table 1
Chemical composition of specimens (mo1%)

Alloy designation	Elements			
	Re	Zr	Ti	Mo
MRZT	15	0.1	0.1	Bal.
MRZ	15	0.1	–	Bal.

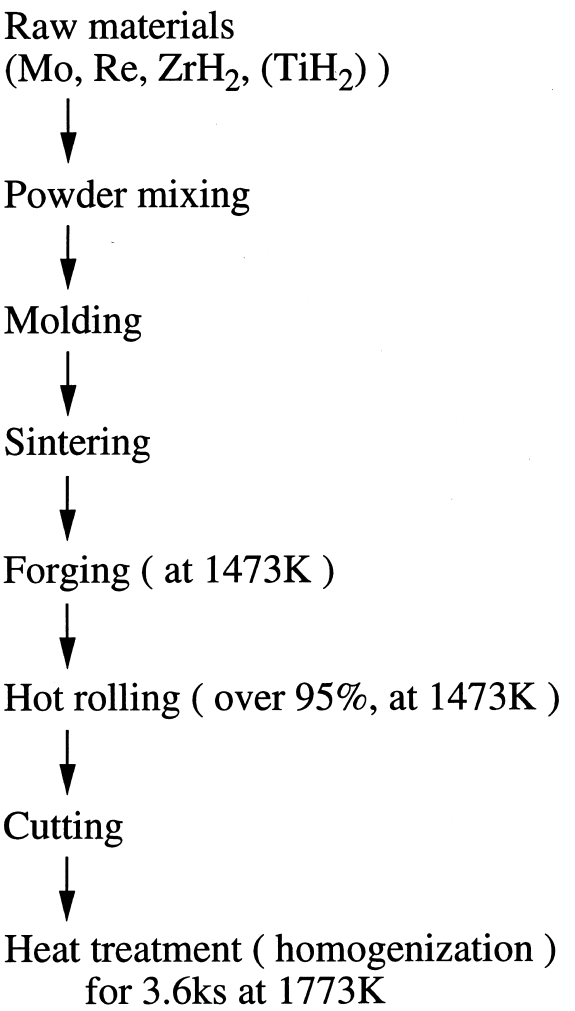

Fig. 1. Alloy production process.

Table 2
Results of the chemical analysis of capsule and specimen holder (Nb–1Zr) (mass%)

Elements				
Zr	Ta	Fe	Si	W
1.0	$\leqslant 0.1$	$\leqslant 0.005$	$\leqslant 0.005$	$\leqslant 0.03$
Ni	Mo	Hf	C	N
$\leqslant 0.005$	$\leqslant 0.005$	$\leqslant 0.02$	$\leqslant 0.01$	$\leqslant 0.01$
O	H	Nb		
$\leqslant 0.015$	$\leqslant 0.001$	Bal.		

Table 3
Results of the chemical analysis of impurities in Li before corrosion test (mass ppm)

Na	Fe	K	Ca	Mg	N
40	10	10	70	10	13

The nitrogen concentration in liquid Li was lower than that of previous experiment [15].

2.3. Micro-analysis on corroded surface

The specimen size was measured accurately using a micrometer prior to corrosion tests. The mass of the specimen was also measured using a high-precision balance before and after corrosion tests. The accuracy of the mass measurement was better than 13 μg. The surface morphology of the specimen was also observed using optical microscopy in the interval of every 0.36 Ms during the corrosion test. After 1.8 Ms, the surface morphology, the microstructure and the composition of corrosion products were examined with the Auger electron spectroscopy and the X-ray diffraction method.

3. Results

3.1. Mass changes due to corrosion in liquid Li

The mass changes with corrosion time are shown in Fig. 2 compared with the previous experimental results [6]. From this figure, it was apparent that all the specimens which were tested in the present experiment showed the mass gain. The amount of the mass gain increased monotonously with increasing corrosion time. The four specimens of the same alloy showed similar corrosion curves, indicating that there was a relatively good reproducibility of the corrosion data obtained in the present experiment. The mass change of the MRZT alloy was larger than that of the MRZ alloy. However, it was still very low, about a half of that of Nb-based alloys [15].

Furthermore all the alloys in this figure showed the mass gain after corrosion test for 0.72 Ms. The mass changes of the present alloys were similar to those of previously tested metal and alloys, despite the difference in the alloy production process between them. The previously tested alloys were prepared by arc-melting in a high purity Ar gas atmosphere, whereas the present alloys were prepared by the powder-metallurgy technique as shown in Fig. 1. Katsuta et al. reported that TZM and pure Mo showed the mass gain when they were held at 873 K for 1018 h (3.66 Ms) in liquid Li (containing 0.1 mass% N) [4], in agreement with the present result. DiStefano reported that pure Mo showed the mass gain, 0.002 g/cm ^{2}, when it was tested at 1270 K for 400 h (1.44 Ms) in liquid Na [5], but the mass loss, −0.011 g/cm ^{2}, when it was tested at 1270 K for 400 h (1.44 Ms) in liquid Li [5], which was inconsistent with the present result. However, the observed mass change of pure Mo and Mo-based alloys (TZM) in those experiments was about ten times smaller than that of pure Nb, pure Ta, pure W, SUS316 and Hastelloy N, all of which were either refractory metals or super-heat resisting alloys. For this reason, it was found that pure Mo and Mo-based alloys showed excellent corrosion resistance in liquid Li.

From Fig. 2, it was evident that the mass gain was dependent largely on the Re content in the alloy. There was a tendency that the amount of mass gain increased with increasing Re content. In fact, lots of corrosion products were formed on the surface of the MRZT alloy (Mo–15mol%Re–0.1mol%Zr–0.1mol%Ti), as shown later in Fig. 6, whereas a very small amount of corrosion products was formed on the surface of pure Mo after corrosion test for 0.72 Ms [6]. Thus, the Re addition into Mo enhanced the formation of the corrosion products, resulting in the larger mass gain. Therefore, in order to understand corrosion behavior of Mo–Re based alloys, it is important to clarify the deposition mechanism of corrosion products.

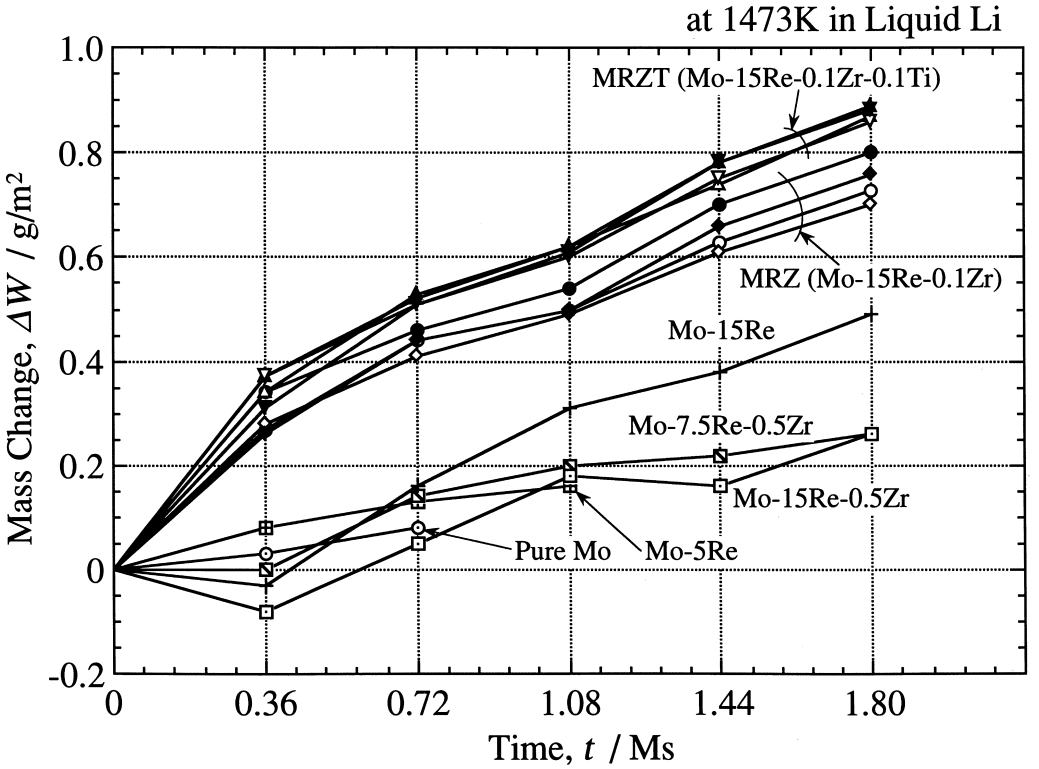

Fig. 2. Mass change of MRZ and MRZT alloys, pure Mo and various Mo-based alloys with corrosion time.

3.2. Evolution of surface morphology with corrosion time

The surface morphology was observed using an optical microscopy at the interval of every 0.36 Ms in the course of corrosion. The morphological evolution of the specimen surface with corrosion time was traced, while focussing our attention on the same area in the surface throughout the observation.

The appearance of the surface on the MRZ alloy is shown in Fig. 3. The traces of polishing flaws were observed on the surface before the corrosion test. However, these were no longer observed in the micrograph of the specimen after the corrosion test for 0.36 Ms, but instead many corrosion products appeared on the surface. They were rough, fine particles with the size of about 5 μm, and distributed over the surface. The mass gain occurred by the adhesion of these corrosion products on the surface. Furthermore, the corrosion products grew up and their number also increased slightly with increasing corrosion time.

The appearance of the surface on the MRZT alloy is shown in Fig. 4. Many corrosion products were observed on the surface even after the short corrosion time of 0.36 Ms. They grew up gradually and their number increased with increasing corrosion time in this MRZT alloy, as was similar to the MRZ alloy. They connected with each other after 0.36 Ms, and finally tended to cover almost all the surface of the specimen. There was a larger amount of corrosion products on the MRZT alloy than that on the MRZ alloy, as might be expected from the larger mass gain in the MRZT alloy than that in the MRZ alloy.

According to our previous study, there were many cracks on the corroded surface in Nb-based alloys [15]. But any cracks were not observed in the present Mo–Re based alloys. Consequently, the Mo–Re based alloys had more excellent corrosion resistance against liquid Li than the Nb-based alloys.

3.3. Micro-analysis of corrosion products with Auger electron spectroscopy

There were two types of corrosion products on the corroded surface of the MRZ alloy as shown in Fig. 5(a). One was a large corrosion product as indicated by A in the figure, and the other was smaller one as indicated by B. The concentration maps of Re, Mo, Zr and N are shown in Fig. 5(b)–(e), respectively. A large amount of Re and a small amount of Zr were detected from the large corrosion product, A, indicating that the Re content in this product was richer than the Zr content. On the other hand, high concentrations of Zr and N were seen on the small corrosion product, B. However, Mo

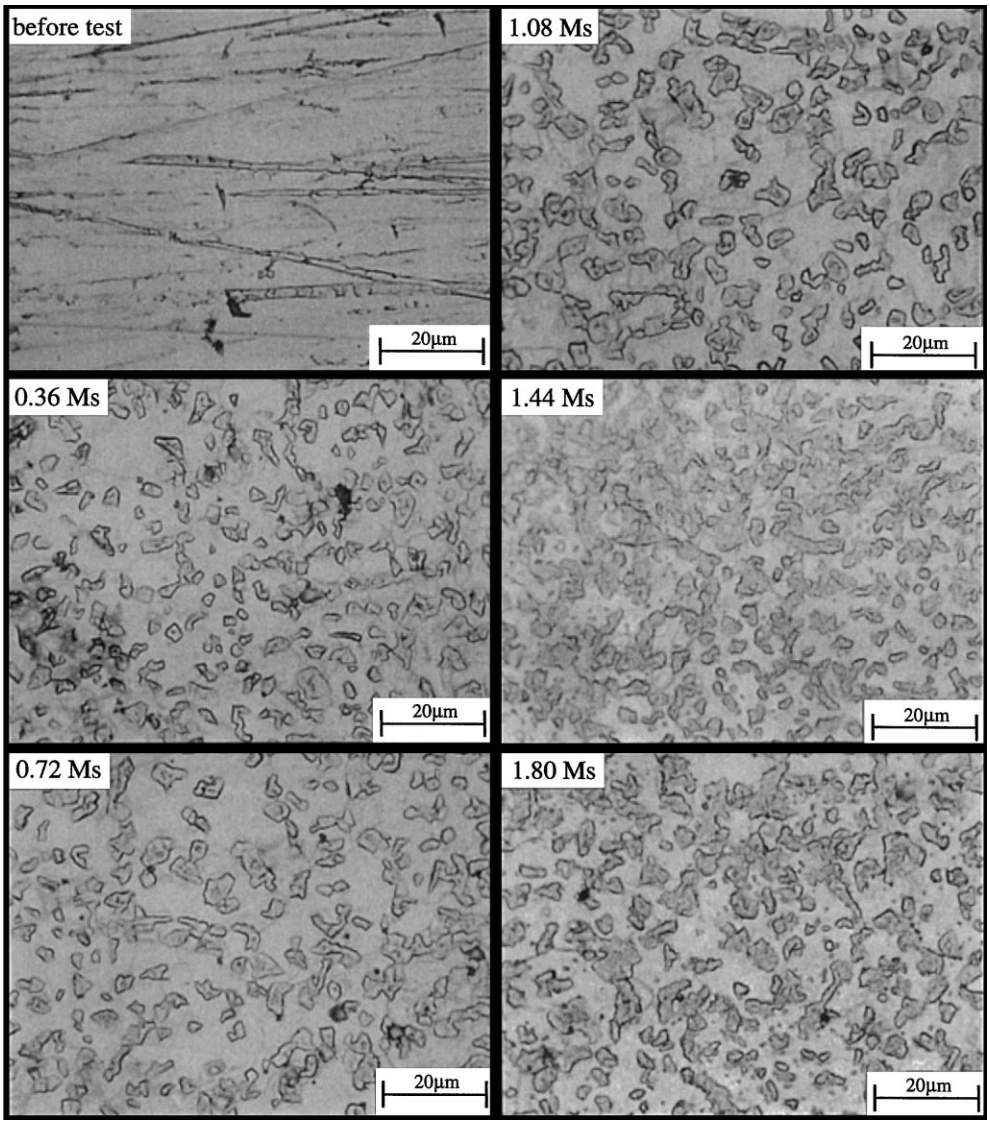

Fig. 3. Evolution of surface morphology for MRZ alloy with corrosion time.

was not detected from both the corrosion products, but it was distributed mainly in the matrix region where any corrosion products did not exist. Thus, Mo did not contribute to the formation of both corrosion products.

A similar result was also obtained from the MRZT alloy as shown in Fig. 6. Titanium was not detected from both the corrosion products, indicating that Ti did not affect the formation of the corrosion products.

3.4. Identification of corrosion products with X-ray diffraction method

The X-ray diffraction patterns are shown in Fig. 7(a) for the MRZ alloy and (b) for the MRZT alloy. The diffraction pattern of the MRZ alloy resembled that of the MRZT alloy. In either pattern, there were many peaks in addition to strong peaks from bcc. Mo. They were identified with the peaks originated from Re_2Zr and ZrN. The Re_2Zr intermetallic compound has a hexagonal structure ($a = 0.52701$ nm and $c = 0.86349$ nm) [16]. This result agreed with the previous experimental results of Mo-based alloys [6]. The ZrN has a cubic structure ($a = 0.457756$ nm) [17]. Furthermore, extra peaks other than from Re_2Zr and ZrN appeared in the X-ray diffraction patterns of both the MRZ and MRZT alloys. However, their intensities were too small to be able to be identified. It was evident from the present results that the large and small corrosion prod-

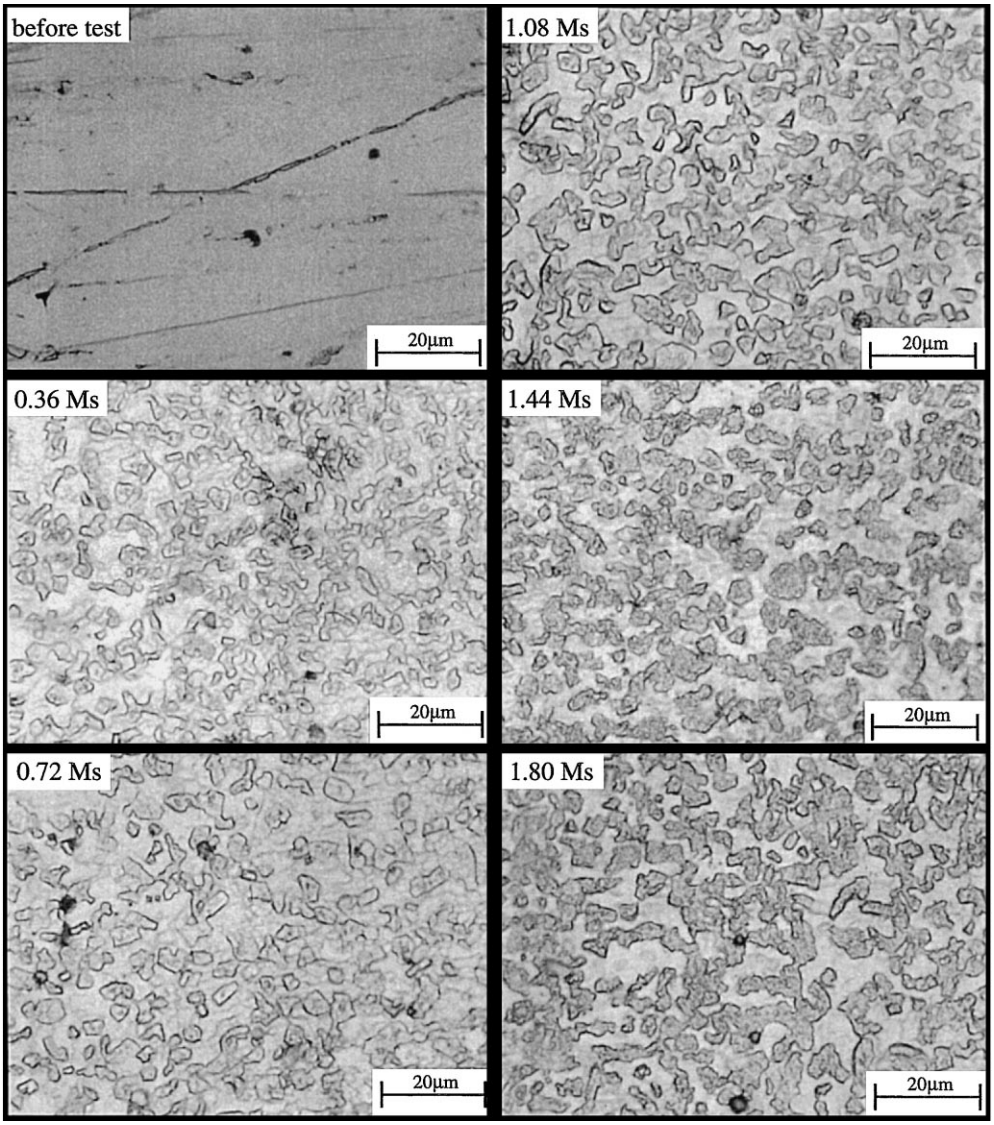

Fig. 4. Evolution of surface morphology for MRZT alloy with corrosion time.

ucts indicated by A and B in Figs. 5(a) and 6(a) were Re_2Zr and ZrN, respectively.

4. Discussion

There were a few experimental results on the deposition mechanism [18–21]. However, there was still no consistent concept of the mechanism in liquid alkali metal. Here, a deposition mechanism of the Mo–Re based alloys was elucidated from our experimental results. The schematic drawing of the deposition mechanism is shown in Fig. 8.

4.1. Dissolution of elements into liquid Li

As shown in Fig. 8(a), metal elements dissolve first into liquid Li. For example, a large amount of Re dissolve into liquid Li during the test at 1473 K. This is confirmed experimentally since the Re concentration in the near-surface region of the specimen surface decreases after corrosion test [6], although the reported solubility of Re is as low as 1mass ppm in Li at the temperature range of 1473–1873 K [22]. It is also known that Zr is dissolved easily into liquid Li, since the solubility of Zr in liquid Li is high [23], for example, 0.00076 mol% at 1073 K to 0.023 mol% at 1473 K [24]. In the present experiment, Zr is dissolved into Li from the capsule and

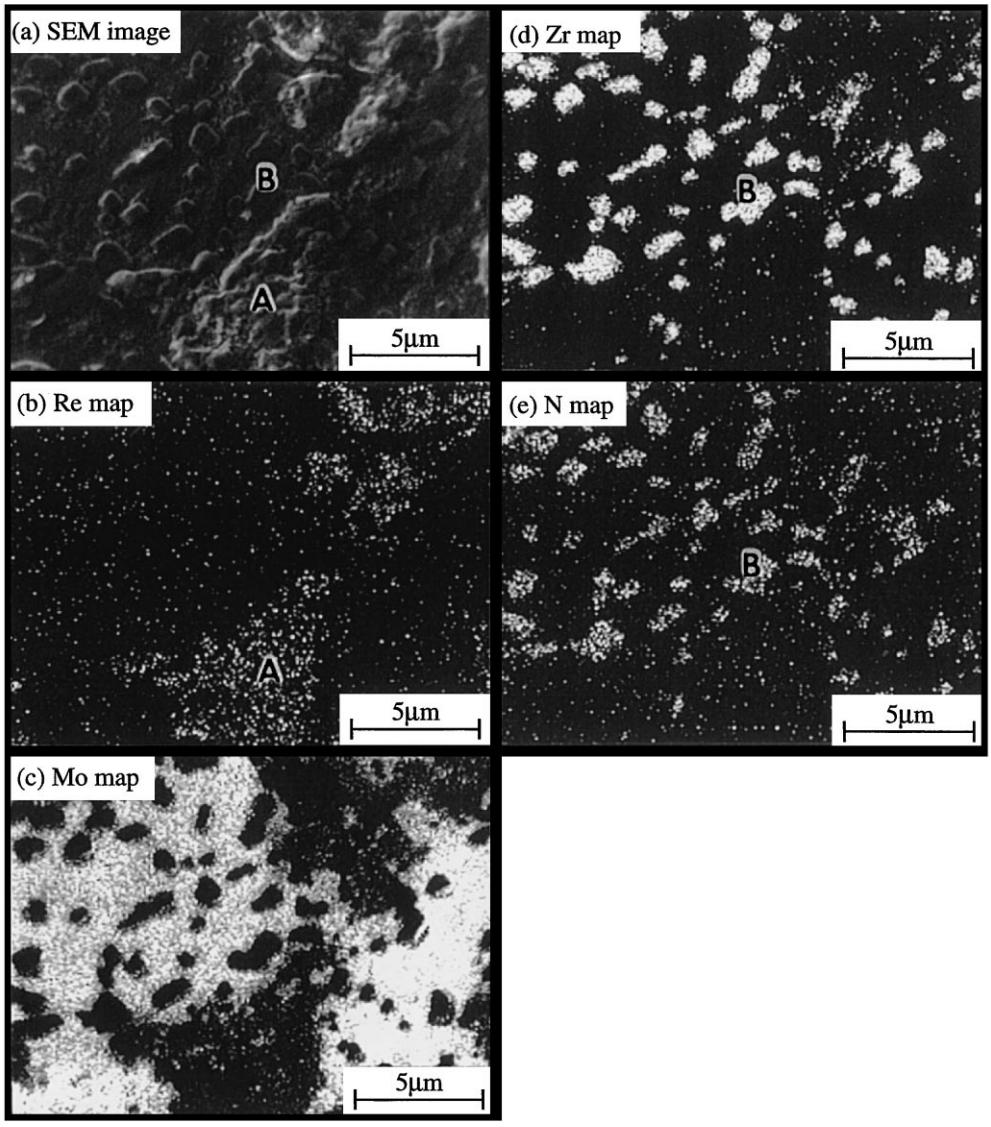

Fig. 5. (a) SEM image, (b) Re, (c) Mo, (d) Zr and (e) N concentration maps on the corroded surface of MRZ alloy measured by an Auger electron spectroscopy.

the specimen holder both of which are made of Nb–1mass%Zr. Molybdenum may be dissolved slightly into liquid Li. But its solubility is lower than that of Zr [25], and hence the dissolution of Mo may be negligibly small in the present case. In addition, nitrogen is contained originally in Li as shown in Table 3. Therefore, as shown in Fig. 8(a), Zr, Re, Mo and N atoms will coexist near the surface of specimen in liquid Li. It is expected that the Re concentration in liquid Li is higher in the vicinity of the specimen surface and it decreases gradually with the distance from the surface. In other words, there is a heterogeneous Re distribution in liquid Li. By contraries, Zr and N may be present homogeneously in liquid Li.

4.2. Deposition of ZrN

Zirconium may react readily with N as shown in Fig. 8(b), because of the very large free energy of formation of ZrN among nitrides [8]. This ZrN compound may deposit on the corroded surface during cooling. In our previous experiment, which has been done in the same corrosion condition as in the present experiment, ZrN has been observed on the surface of binary Nb-based alloys [7]. DeStefano also reported that ZrN was detected in the cold zone region of Nb–1Zr loop [5]. For these reasons, ZrN compound was supposed to deposit even on the corroded surface of Mo-based alloys. However, the amount of ZrN was less than that of Re_2Zr

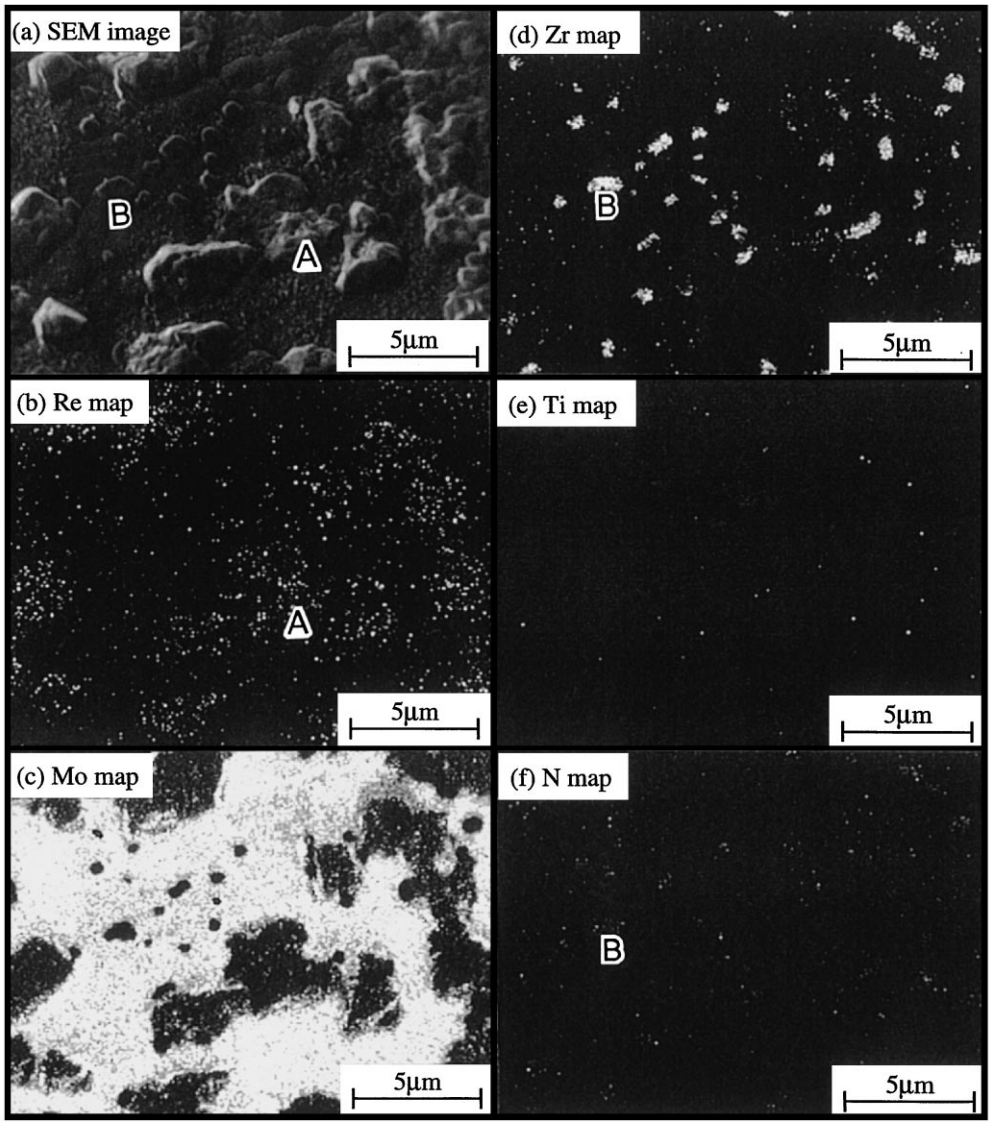

Fig. 6. (a) SEM image, (b) Re, (c) Mo, (d) Zr, (e) Ti and (f) N concentration maps on the corroded surface of MRZT alloy measured by an Auger electron spectroscopy.

on the corroded surface, because of the low nitrogen concentration in liquid Li. The nitrogen concentration, 13 ppm, in liquid Li used in the present experiment was much lower than those in the previous experiment, 30 and 90 ppm [15]. Hence, the total amount of ZrN was smaller in the present experiment than in the previous one. In fact, the measured X-ray diffraction pattern peak intensities from ZrN were much weaker in the present experiment than in the previous one.

4.3. Deposition of Re_2Zr

After the deposition of ZrN, Re, Mo and Zr will still remain in liquid Li. The concentration near the specimen surface in liquid Li may change in the order, Re - $\gg$ Zr $\gg$ Mo. If this is the case, Re-rich precipitates may be formed preferentially. According to the Re–Zr and the Re–Mo binary phase diagrams, there are many intermetallic compounds, i.e., $Re_{24}Zr_5$, Re_2Zr, $ReZr_2$, χ phase (Mo–75.6–78mol%Re) and σ phase (Mo–55–70mol%Re). Also, the solubility of Zr in Re is about 1.5 mol% (at 1473 K), which is much lower than the solubility of Mo in Re, 8 mol% at 1473 K. Consequently, Re–Zr compounds are expected to be formed more easily than Re–Mo compounds. Among the Re–Zr compounds, Re_2Zr may be most stable, judging from its highest melting temperature, 3023 K, and hence it precipitates easily in liquid Li and deposits on the corroded

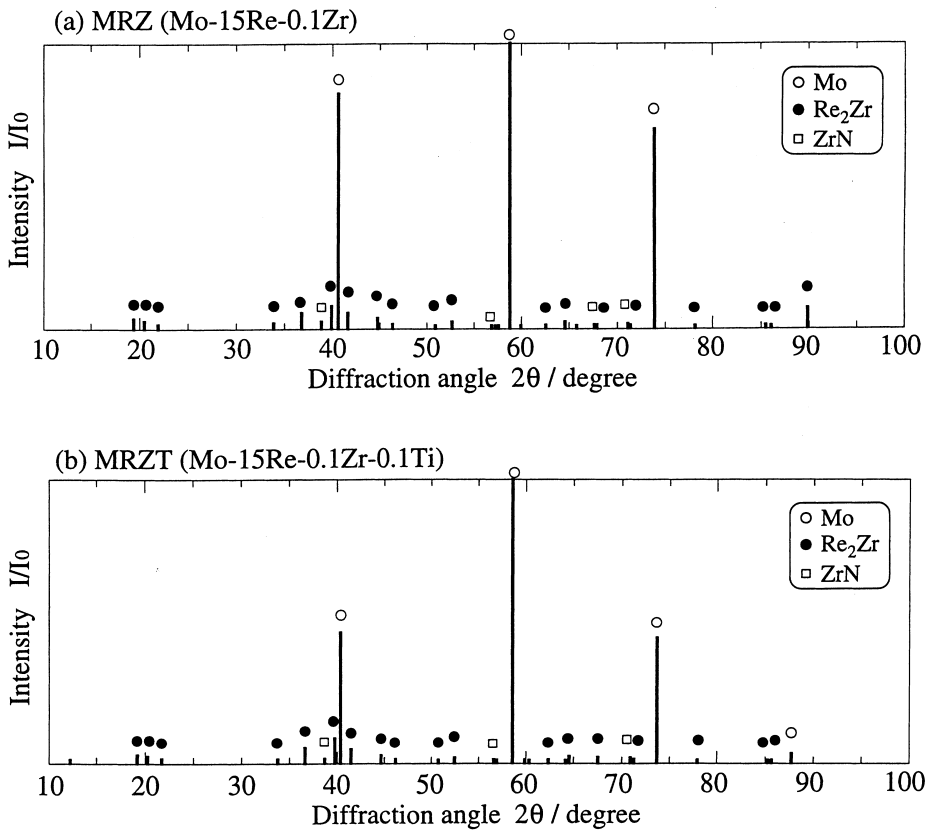

Fig. 7. X-ray diffraction patterns of (a) MRZ and (b) MRZT alloys, obtained after corrosion test in liquid Li at 1473 K for 1.8 Ms. The X-rays used were Cu Kα radiation.

surface, as was found in the present experiment of the AES shown in Figs. 5 and 6 and also of the X-ray diffraction pattern shown in Fig. 7.

Although the dissolution of Re into liquid Li causes the mass loss of the alloy, the dissolved Re in liquid Li is redeposited on the corroded surface by forming Re_2Zr. As a result, all the specimens exhibited the mass gain after corrosion test, as shown in Fig. 2.

Thus, a sort of chemical reaction takes place primarily between non-metallic and metallic elements in liquid metal. This reaction is dependent largely on the free energy of formation of the products. Then, the corrosion products which consist of metallic and non-metallic elements deposit on the specimen surface. Subsequently, another reaction takes place between the residual metallic elements in liquid Li, and some corrosion products (i.e., intermetallic compounds) are formed. In this reaction, both the concentration of metallic elements and the liquid Li temperature are very important factors for controlling the formation of corrosion products. Needless to say, the most stable compound at a given temperature precipitates as a corrosion product in liquid metal and deposits on the corroded surface. Barker et al. reported that the composition of corrosion products was dependent largely on the temperature of SUS316 type loop [19]. Also, Yokota et al. investigated the deposition process using a sodium loop, and showed that what kind of products deposited on the surface was predictable from binary phase diagrams [18]. Such an approach is useful even in the present case, as explained earlier.

5. Conclusion

The corrosion behavior was investigated in liquid Li at 1473 K for two Mo–Re based alloys, MRZ and MRZT, which were designed as new structural materials for advanced atomic power plants. The mass gain of the MRZT alloy due to the corrosion was larger than that of the MRZ alloy, but it was much less than that of the Nb-based alloys. Also, there were no cracks on the surface of either alloy after the corrosion test for 1.8 Ms. Therefore the designed Mo–Re based alloys were superior in the corrosion resistance against liquid Li to the Nb-based alloys (i.e., Nb–1Zr).

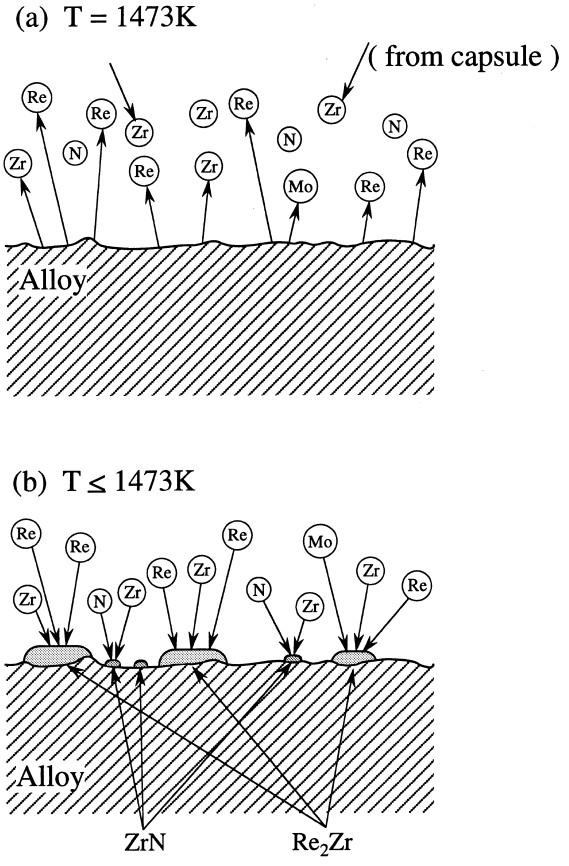

Fig. 8. Schematic drawings of deposition mechanism for Mo–Re based alloys.

There were two types of corrosion products on the corroded surface. One was Re_2Zr, and the other was ZrN. The deposition mechanism of these corrosion products was proposed on the basis of their free energy of formation, phase diagram as well as the concentration of elements in liquid Li.

Acknowledgements

The authors would like to express sincere thanks to S. Inoue, Numazu College of Technology, for his valuable help throughout this study.

References

[1] E. Pink, Int. J. Refract. Met. Hard Mater. 5 (1986) 192.
[2] H.A. Calderon, G. Kostorz, G. Ullrich, Mater. Sci. Eng. A 160 (1993) 189.
[3] A. Luo, J.J. Park, D.L. Jacobson, B.H. Tsao, M.L. Ramalingam, Mater. Sci. Eng. A 177 (1994) 89.
[4] H. Katsuta, K. Furukawa, J. Nucl. Mater. 71 (1977) 95.
[5] J.R. DiStefano, J. Mater. Eng. 11 (1989) 215.
[6] S. Inoue, J. Saito, S. Kano, K. Manabe, M. Furui, M. Morinaga, in: Abs. Int. Symp. on Advanced Materials and Technology for the 21th Century, Honolulu, The Japan Institute of Metals, 1995, p. 194.
[7] D.L. Smith, K. Natesan, Nucl. Technol. 22 (1974) 392.
[8] R.L. Klueh, Metall. Trans. 5 (1974) 875.
[9] J.H. DeVan, R.L. Klueh, Nucl. Technol. 24 (1974) 64.
[10] J. Saito, S. Inoue, S. Kano, M. Furui, M. Morinaga, in: G. Kneringer, P. Rodhammer, P. Wilhartitz, Proceedings of the 14th Int. PLANSEE Sem.'97, 1997, p. 805.
[11] J. Saito, M. Morinaga, S. Kano, M. Furui, M. Oda, to be published.
[12] W.D. Klopp, W.R. Witzke, Metall. Trans. 4 (1973) 2006.
[13] N. Igata, A. Kohyama, K. Itadani, J. Nucl. Mater. 85&86 (1979) 895.
[14] Y. Hiraoka, S. Yoshimura, K. Takebe, Int. J. Refract. Metals Hard Mater. 12 (1994) 261.
[15] J. Saito, S. Inoue, S. Kano, T. Yuzawa, M. Furui, M. Morinaga, J. Nucl. Mater., to be submitted (1998).
[16] N.H. Krikorian, W.G. Witteman, M.G. Bowman, J. Phys. Chem. 64 (1960) 1517.
[17] Nat. Bur. Stand. (US) Monogr. 21 (1984) 16.
[18] N. Yokota, S. Shimoyashiki, J. Japan Inst. Met. 52 (1988) 320.
[19] N. Yokota, S. Shimoyashiki, J. Japan Inst. Met. 53 (1989) 175.
[20] M.G. Barker, M.J. Capaldi, in: H.U. Borgstedt, G. Frees (Eds.), Liquid Metal Systems, Plenum, New York, 1995, p. 105.
[21] V.A. Ivanov, Y.N. Afonina, V.A. Soloviev, J. Nucl. Mater. 233–237 (1996) 581.
[22] R.L. Eichelberger, R.L. McKisson, B.G. Johnson, Solubility studies of refractory metals and alloys in potassium and lithium, USAEC Report A1-68-110, 1968.
[23] C.E. Session, J.H. DeVan, Nucl. Appl. Tech. 9 (1970) 250.
[24] Yu.F. Bychkov, A.N. RoZanov, V.B. Yakovleva, Soviet Atomic Energy 7 (1960) 987. [Trans. from Atomnaya Energiya 7 (6), 581].
[25] H.W. Leavenworth, R.E. Cleary, Acta Metallurgica 9 (1961) 519.